Unifying the Low-Temperature Photoluminescence Spectra of Carbon Nanotubes: The Role of Acoustic Phonon Confinement

F. Vialla,[1] Y. Chassagneux,[1,*] R. Ferreira,[1] C. Roquelet,[2] C. Diederichs,[1] G. Cassabois,[3] Ph. Roussignol,[1] J. S. Lauret,[2] and C. Voisin[1]

[1]*Laboratoire Pierre Aigrain, École Normale Supérieure, CNRS (UMR 8551), Université Pierre et Marie Curie, Université Paris Diderot, 24, rue Lhomond, F-75005 Paris, France*

[2]*Laboratoire Aimé Cotton, École Normale Supérieure de Cachan, Université Paris Sud, CNRS (UPR3321), F-91405 Orsay, France*

[3]*Laboratoire Charles Coulomb, Université de Montpellier, CNRS (UMR5221), F-34095 Montpellier, France*

(Received 3 December 2013; published 30 July 2014)

At low temperature the photoluminescence of single-wall carbon nanotubes show a large variety of spectral profiles ranging from ultranarrow lines in suspended nanotubes to broad and asymmetrical line shapes that puzzle the current interpretation in terms of exciton-phonon coupling. Here, we present a complete set of photoluminescence profiles in matrix embedded nanotubes including unprecedented narrow emission lines. We demonstrate that the diversity of the low-temperature luminescence profiles in nanotubes originates in tiny modifications of their low-energy acoustic phonon modes. When low-energy modes are locally suppressed, a sharp photoluminescence line as narrow as 0.7 meV is restored. Furthermore, multipeak luminescence profiles with specific temperature dependence show the presence of confined phonon modes.

DOI: 10.1103/PhysRevLett.113.057402 PACS numbers: 78.67.Ch, 63.22.Gh, 78.55.-m

Single-wall carbon nanotubes (SWNTs) are fascinating nanostructures with unique properties that make them promising for a number of optoelectronic applications. The understanding of their basic photophysical properties has been the focus of an intense research effort with major leaps such as the measurement of an exceptional exciton binding energy [1], the detection of trions and biexcitons [2,3], or the observation of photon antibunching due to the localization of excitons [4]. In contrast, the understanding of the low-temperature photoluminescence (PL) spectra of carbon nanotubes remains a pending issue, with apparently inconsistent results reported in the literature. For instance, the low-temperature luminescence profiles of SWNTs range from broad (more than 10 meV) and asymmetrical lines to narrow (less than 40 μeV) and symmetrical lines [5–9].

The general framework of the coupling of a localized exciton to an acoustic phonon bath was developed by Krummheuer *et al.* [10]. In the case of nanotubes, Galland *et al.* [7] showed that this model predicts intrinsically broad and asymmetrical line shapes. This so-called Ohmic model accounts for a limited set of luminescence profiles but fails to explain the variety of profiles reported in the literature. In this model, the red shifted (respectively, blue shifted) wing of the PL line corresponds to the radiative recombination of the exciton assisted by the emission (respectively, absorption) of an acoustic phonon. In contrast to the case of epitaxial quantum dots embedded in a three-dimensional phonon bath where a sharp purely electronic zero phonon line (ZPL) accompanied by weak phonon sidebands is observed [11,12], a strong prediction of this model in the case of a 1D phonon bath is the complete merging of the ZPL into the phonon wings [13]. Thus, for a 1D phonon bath, the dominant optical process near the electronic resonance is the simultaneous emission of a photon and a phonon. As a consequence, the photoluminescence line shape is driven by this nonperturbative coupling to long wavelength acoustic phonons rather than by the eigen properties of the electronic two-level system. This peculiar exciton-phonon coupling provides a new means to probe the coupling between exciton and low-energy acoustic phonons with an unprecedented sensitivity.

In this Letter, we present a complete set of PL spectra spanning a large variety of profiles and line widths. We show that, due to phonon confinement, the coupling of excitons to acoustic phonons can deviate strongly from the Ohmic regime especially for phonon energies lower than a few meV. This has drastic effects on the photoluminescence spectra recovering a sharp ZPL. Phonon confinement allows us to explain all the observed spectra both for matrix embedded and suspended SWNTs, provided that the much longer dephasing time of suspended nanotubes is properly taken into account.

The PL spectra were recorded on individual SWNTs using a homemade confocal microscope. The surfactant (sodium cholate) embedded CoMoCat SWNTs were deposited onto the flat surface of a high refractive index solid immersion lens to improve the excitation and collection efficiencies. Prior to SWNTs deposition, the solid immersion lens was functionalized with a poly-L-lysine layer to increase the linkage of the micelles to the substrate.

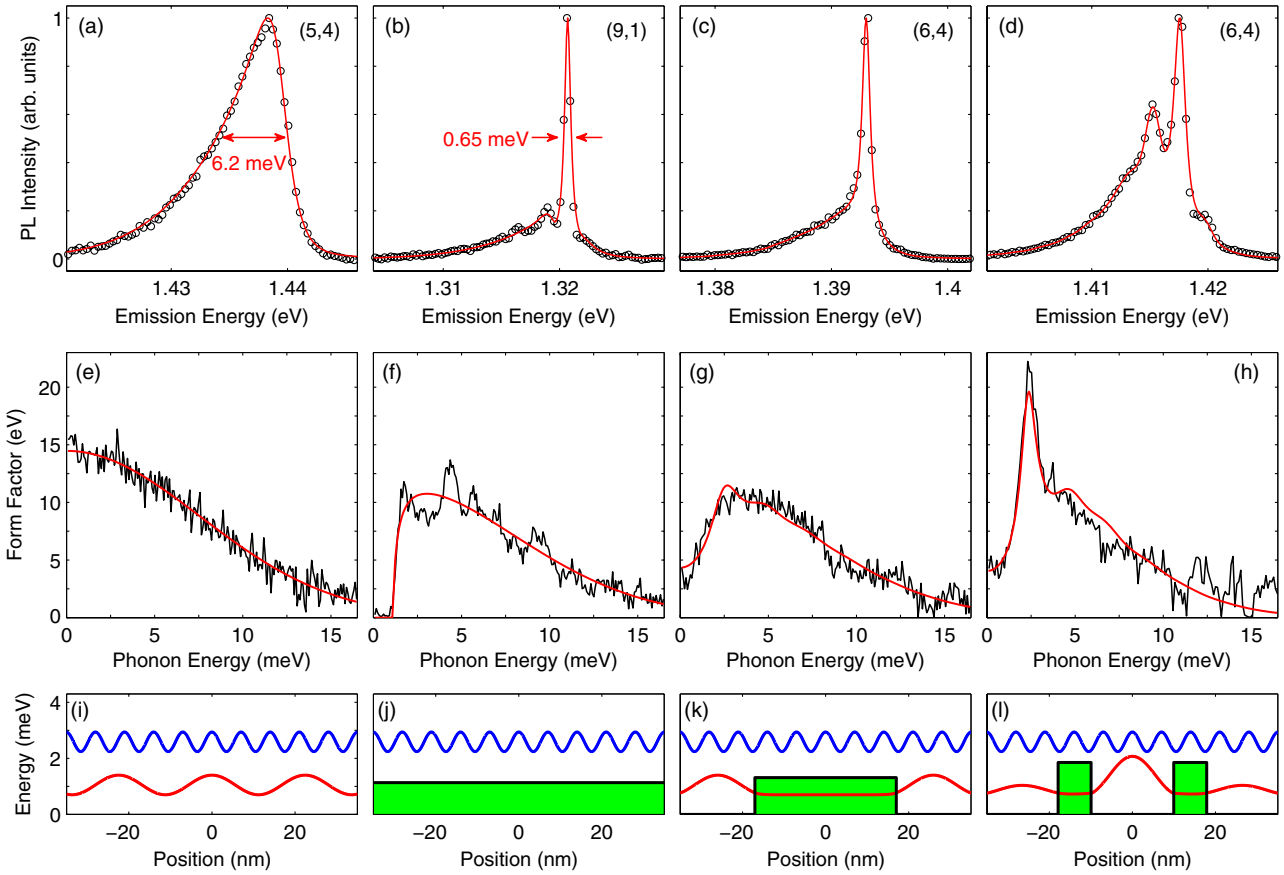

FIG. 1 (color online). (a)–(d) PL spectra of individual SWNTs recorded at 10 K (open dots). Chiral species are indicated in parentheses. The red solid lines are simulated spectra using the fit of the form factor of panels (e)–(h). (e)–(h) Form factors (see text) extracted from the corresponding spectra. The continuous lines are fits to the acoustic barrier model [13]. (i)–(l) Schematic representation of two exemplary local phonon modes [$\hbar\omega = 1$ meV (red line) and $\hbar\omega = 2.5$ meV (blue line)] resulting from the presence of acoustic barriers (depicted as filled green rectangular profiles). For the spectrum simulation, the exciton is supposed to be located at $z = 0$.

The sample was placed on the cold finger of an optical helium cryostat. Optical excitation was performed with a cw Ti:sapphire laser with intensities of 1 kW/cm^2 or below. Exposure times of typically one minute were used.

Figures 1(a)–1(d) show the typical low-temperature PL profiles observed in our samples. The first one, Fig. 1(a), consists of an asymmetrical profile and is similar to those reported by Galland *et al.* [7]. The second one, Fig. 1(b), exhibits a sharp peak onto an asymmetrical pedestal. Note that this kind of profile is closer to the ones observed for suspended SWNTs [5,6]. We also found a continuous set of spectra [such as in Fig. 1(c)] bridging the narrow and the broad ones. Finally, the last example, Fig. 1(d), shows a multipeak feature onto an asymmetrical pedestal.

In fact, we note that the pedestal [Figs. 1(b)–1(d)] has—in all spectra—a shape and a width (a few meV) comparable to that of the asymmetrical spectrum [Fig. 1(a)]. The temperature dependence of the PL line shape of the tubes shown in Figs. 1(c) and 1(d), is given in Fig. 2 and shows striking similarities: when raising the temperature, the blue wing tends to increase leading to a symmetrized profile. Importantly, we found that the relative height of the red and blue side peaks in Fig. 1(d) fits to a Boltzmann factor with an activation energy of 2.5 meV equal to the splitting between the peaks [13]. This rules out that these peaks would arise from spectral diffusion. Actually, spectral diffusion would not lead to such temperature dependence since there is no simple relationship between the trapping energy of a charge and the magnitude of the related Stark shift [13]. More generally, we managed to fit the relative weight of the blue and red wings to a Boltzmann factor for all spectra, showing that these wings are related to phonon assisted processes [13]. Thus, we speculate that all the PL profiles originate from the coupling of excitons to phonons.

In order to extract the coupling between the exciton and acoustic phonons, we used the calculations developed for semiconductor quantum dots in [10] and that were adapted for SWNTs in [7]. We assume that excitons couple only to the 1D acoustic phonons of the nanotube due to the strong sound velocity mismatch between the nanotube ($v \simeq 2 \times 10^4$ m/s) and the substrate ($\simeq 3 \times 10^3$ m/s). In carbon nanotubes, three acoustic phonon branches are

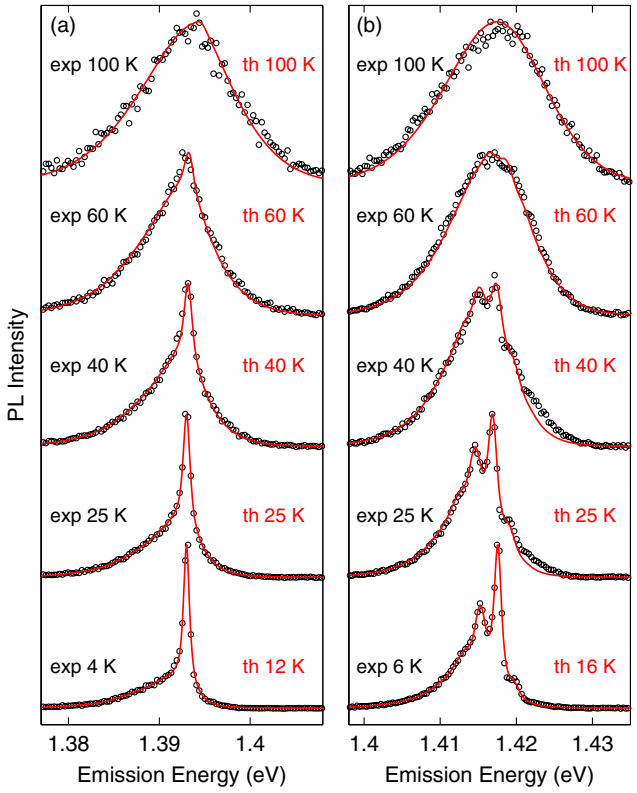

FIG. 2 (color online). Evolution of the normalized PL spectra (vertically shifted for clarity) as a function of temperature (black open dots). (a) (respectively (b)) for the nanotube of [Fig. 1(c)] (respectively [Fig. 1(d)]). The red solid lines are the spectra calculated from the extracted form factor at the lowest temperature [Figs. 1(e)–1(h)]. The measured base plate temperature is indicated together with the effective temperature used for the fitting.

coupled to the exciton: the stretching, twisting, and radial breathing modes [14,15]. The acoustic phonons couple to excitons through the difference of the off-diagonal terms of the deformation potential for electrons and holes $D = D_e - D_h$. Because of the complementary dependences with the chiral angle, the different branches can be merged into an effective acoustic mode [16]. The exciton-phonon coupling matrix element is given by [10]

$$\hbar g(\omega) = \sqrt{\frac{\hbar\omega}{2\rho L v^2}} F(\omega). \quad (1)$$

L is the nanotube length, ρ is the linear mass density, v is the sound velocity, $\hbar\omega$ is the energy of the phonon mode. and $F(\omega)$ is a form factor. In the case of a perfectly 1D acoustic mode, one has $F = F_0$ (Ohmic coupling) with

$$F_0(\omega) = D \int dz |\psi(z)|^2 e^{iqz}, \quad (2)$$

where $\psi(z)$ is the exciton center-of-mass envelope wave function and where $\omega = v|q|$. Note that in this Ohmic model one has $F_0(0) = D$ regardless of the exciton wave function, which leads to the merging of the ZPL into the phonon wings. In the case of a Gaussian exciton envelope, $\psi(z) = (1/\pi^{1/4}\sigma^{1/2}) \exp(-(z^2/2\sigma^2))$, where σ is the exciton localization length, the form factor reads

$$F_0(\omega) = D \exp[-(\omega\sigma/2v)^2]. \quad (3)$$

This implies a high energy cutoff of the exciton-acoustic phonon coupling at $\hbar\omega_\sigma \approx 2\hbar v/\sigma$ that simply results from momentum conservation within the width of the exciton envelope in the k space.

The emission spectra can be computed from the coupling matrix element by summing up the contributions of all phonon modes weighted by their occupation numbers [7,10]. Conversely, the form factor $F(\omega)$ can be traced back from the experimental spectra with the procedure described in [13]. The form factor extracted from the broad and asymmetric profile is presented in Fig. 1(e). This form factor fits well to a Gaussian such as F_0, as expected in the Ohmic model [7].

Even if the experimental spectra show a large variety of profiles [Figs. 1(a)–1(d)], the extracted form factors share common features. Importantly, we note that they do not depend on the temperature (as expected from the model). In addition, all the form factors display a Gaussian baseline, from which we can extract a deformation potential D between 12 and 15 eV, and an exciton localization length σ of around 3 nm, similar to the ones found in [7]. The main deviation from the Ohmic coupling occurs for low phonon energies, typically below 3 meV. For instance the narrow spectrum of Fig. 1(b) corresponds to a complete suppression of the coupling [$F(\omega) = 0$] for low-energy phonons [Fig. 1(f)]. Again, we stress that this reduced coupling cannot be accounted for by a modification of the exciton wave function within the Ohmic model, since the form factor goes to D for vanishing ω regardless of the envelope shape [Eq. (2)]. In terms of the emission spectrum, this means that changing the exciton envelope function (shape or localization length) cannot account simultaneously for the observed narrow ZPL (requiring a delocalized exciton) and a broader pedestal (requiring a tightly localized exciton). Therefore, the low-energy modification of the form factor must arise from the phonon modes themselves (as discussed at the end of the Letter).

The key to the understanding of the strong variations of the PL line shapes actually lies in the low-energy exciton-phonon coupling. When F takes sizable values for vanishing phonon energies, the ZPL is strongly suppressed to the profit of the phonon wing. In contrast, if the form factor is reduced for low phonon energies ($\omega < \omega_c$) a sharp ZPL is restored [Fig. 1(b)]. Practically, this effect is observable if the cutoff phonon energy $\hbar\omega_c$ is greater than the natural line width of the ZPL: $\omega_c > 2/T_2$, where T_2 is the ZPL dephasing time. Experimentally, we found a width of $\approx$0.65 meV for the ZPL and $\hbar\omega_c \approx 1.2$ meV in Fig. 1(b),

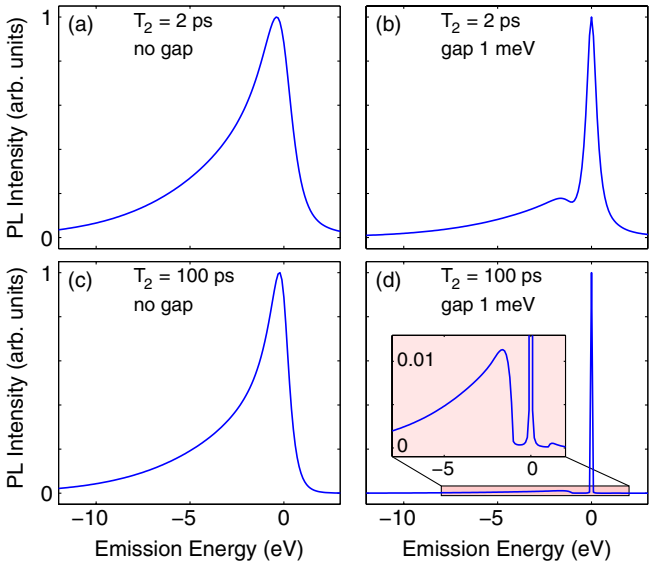

FIG. 3 (color online). Calculated spectrum for the Ohmic coupling [panels (a) and (c)] and for a 1 meV gap in the coupling [panels (b) and (d)]. Spectrum are calculated assuming a dephasing time T_2 of 2 ps [panels (a) and (b)], and for $T_2 =$ 100 ps [panels (c) and (d)]. All the other parameters are identical for the four plots ($T = 5$ K, $D = 13$ eV, and $\sigma = 3$ nm).

which explains why the phonon sideband and the ZPL are not completely split off.

More generally, the effect of the dephasing time on the spectral line shape is presented in Fig. 3. In the case of the Ohmic coupling, the line shape is roughly insensitive to the value of the electronic dephasing time. This is a peculiarity of the 1D geometry, where the ZPL is completely merged into the phonon wings. In the case of a low-energy gap in the form factor (in Fig. 3 we used a 1 meV gap), a sharp ZPL is restored. The amplitude of the ZPL is directly proportional to the dephasing time T_2 since the area of the line must be constant, reflecting the conservation of the oscillator strength of the transition. In contrast, the phonon wings hardly depend on T_2. Longer dephasing times such as those observed in suspended nanotubes therefore lead to an apparent magnification of the ZPL. For example in Fig. 1 of [5], a sharp ZPL and a weak phonon sideband are observable [17]. The ZPL to sideband amplitude ratio is of the order of 100 for a ZPL width of 40 μeV. Consistently, the spectrum displayed in Fig. 1(b) shows a ratio of the order of 5, for a ZPL width of 650 μeV.

We note that some suspended NT spectra have no apparent phonon wings. We believe that this is due to experimental limitations. In fact, reaching a given signal to noise ratio requires much shorter integration times for sharp ZPLs, which may lose the weak sidebands in the noise background [18].

Let us now examine possible origins of the reduction of the coupling to the low-energy phonon modes. Equivalently, this low-energy cutoff can be seen as a reduction of the low-energy phonon density of states probed by the exciton. Generally speaking, such local modifications of the phonon modes can be accounted for by introducing acoustic barriers, with height $\hbar\omega_c \simeq 2$ meV [13]. Actually, since 1D structures are much more sensitive to perturbations than their higher dimension counterparts, several ordinary effects may cause important phonon modifications. In the case of suspended SWNTs, amorphous carbon deposited by places or structural defects can break the 1D translational symmetry, leading to low-energy phonon modifications [19]. In the case of embedded SWNTs, the noncovalent contact to the substrate or matrix is known to occur on nanometer scale zones [20] and leads to the opening of few-meV-phonon gaps [21] due to a local hardening of the nanotube lattice.

The different types of PL profiles then arise from different geometries of the barrier. We make use of the general expression for the form factor F

$$F(\omega_i) = D\sqrt{L}\, v/\omega_i \int dz |\psi(z)|^2 W_i'(z), \qquad (4)$$

where $W_i(z)$ are the orthonormal acoustic modes, solutions of

$$-\omega_i^2 W_i(z) = v^2 W_i''(z) - \omega_b^2(z) W_i(z). \qquad (5)$$

For the sake of simplicity, we assume here that the acoustic barrier amplitude $\hbar\omega_b(z)$ is either 0 or $\hbar\omega_c$ along the nanotube [Figs. 1(i)–1(l)]. Without a barrier, free propagating modes are obtained and $F = F_0$ [Figs. 1(a) and 1(e)]. If the barrier width is much larger than the exciton localization length, a true gap is found in the form factor [Figs. 1(b) and 1(f)]. For an intermediate barrier width, typically a few tens of nanometers, the coupling is only partially canceled, owing to the finite attenuation length of the evanescent low-energy phonon modes inside the barrier [Figs. 1(c) and 1(g)] [13].

An additional case of interest corresponds to the situation where the exciton is located between two acoustic barriers separated by a few tens of nanometers. Our model predicts that in this case side peaks should appear in the phonon wing because the exciton is coupled to a resonant vibration mode between the barriers. We actually found experimental evidence for such resonant coupling [Figs. 1(d) and 1(h)]. The observed splitting (2.5 meV) corresponds to a distance between the barriers of the order of 20 nm, consistent with the scale of variations of the environment of the nanotube. This original observation corresponds to the interesting situation of disorder-induced confinement of vibrations at the nanoscale.

In conclusion, the low-temperature PL profiles of carbon nanotubes (ranging from sharp sub-meV lines to broad asymmetrical lines) are well accounted for within a single model describing the coupling of a localized exciton and a one-dimensional phonon bath. The key to the diversity of

the profiles lies in tiny modifications of the low-energy phonons. The observation of a narrow line shape indicates the presence of a gap in the exciton-phonon coupling. Furthermore, we pointed out the key role of the ZPL dephasing rate in the overall profile of the PL, explaining the apparent discrepancy between suspended and embedded nanotubes. This reduction of the coupling to acoustic phonons is a first important step towards the control of the emission line width of matrix embedded carbon nanotubes. Finally, we showed that phonons may be confined by disorder with specific fingerprints in the PL spectrum.

This work was supported by the GDR-I GNT, the grant "C'Nano IdF TENAPO." C. V. and G. C. are members of "Institut Universitaire de France."

*yannick.chassagneux@lpa.ens.fr

[1] F. Wang, G. Dukovic, L. E. Brus, and T. F. Heinz, Science **308**, 838 (2005).
[2] R. Matsunaga, K. Matsuda, and Y. Kanemitsu, Phys. Rev. Lett. **106**, 037404 (2011).
[3] L. Colombier, J. Selles, E. Rousseau, J. S. Lauret, F. Vialla, C. Voisin, and G. Cassabois, Phys. Rev. Lett. **109**, 197402 (2012).
[4] A. Högele, C. Galland, M. Winger, and A. Imamoglu, Phys. Rev. Lett. **100**, 217401 (2008).
[5] M. S. Hofmann, J. T. Gluckert, J. Noe, C. Bourjau, R. Dehmel, and A. Högele, Nat. Nanotechnol. **8**, 502 (2013).
[6] I. Sarpkaya, Z. Zhang, W. Walden-Newman, X. Wang, J. Hone, C. W. Wong, and S. Strauf, Nat. Commun. **4**, 2152 (2013).
[7] C. Galland, A. Högele, H. E. Türeci, and A. Imamoğlu, Phys. Rev. Lett. **101**, 067402 (2008).
[8] J. Lefebvre, P. Finnie, and Y. Homma, Phys. Rev. B **70**, 045419 (2004).
[9] H. Htoon, M. J. O'Connell, P. J. Cox, S. K. Doorn, and V. I. Klimov, Phys. Rev. Lett. **93**, 027401 (2004).
[10] B. Krummheuer, V. M. Axt, and T. Kuhn, Phys. Rev. B **65**, 195313 (2002).
[11] L. Besombes, K. Kheng, L. Marsal, and H. Mariette, Phys. Rev. B **63**, 155307 (2001).
[12] I. Favero, G. Cassabois, R. Ferreira, D. Darson, C. Voisin, J. Tignon, C. Delalande, G. Bastard, P. Roussignol, and J. M. Gerard, Phys. Rev. B **68**, 233301 (2003).
[13] See Supplemental Material at http://link.aps.org/supplemental/10.1103/PhysRevLett.113.057402 for details.
[14] H. Suzuura and T. Ando, Phys. Rev. B **65**, 235412 (2002).
[15] G. Pennington and N. Goldsman, Phys. Rev. B **71**, 205318 (2005).
[16] D. T. Nguyen, C. Voisin, P. Roussignol, C. Roquelet, J. S. Lauret, and G. Cassabois, Phys. Rev. B **84**, 115463 (2011).
[17] Ultranarrow PL spectra of suspended nanotubes at 4 and 77 K provided by A. Hoegele in a private communication could be quantitatively fitted to our model with an acoustic barrier width of 80 nm and height of 1 meV.
[18] In some other cases where no antibunching signature is observed [6], the exciton could be more delocalized, which would also suppress the wings.
[19] We note that self-trapping of the exciton with the acoustic phonon can also lead to a modification of the phonon spectrum in the meV range [22].
[20] J. J. Crochet, J. G. Duque, J. H. Werner, B. Lounis, L. Cognet, and S. K. Doorn, Nano Lett. **12**, 5091 (2012).
[21] A. V. Savin, B. Hu, and Y. S. Kivshar, Phys. Rev. B **80**, 195423 (2009).
[22] P. B. Shaw and E. W. Young, Phys. Rev. B **24**, 714 (1981).